

Efficient Collocational Approach for Parametric Uncertainty Analysis

Dongbin Xiu*

Department of Mathematics, Purdue University, West Lafayette, IN 47906, USA.

Received 23 February 2006; Accepted (in revised version) 18 June 2006

Available online 30 September 2006

Abstract. A numerical algorithm for effective incorporation of parametric uncertainty into mathematical models is presented. The uncertain parameters are modeled as random variables, and the governing equations are treated as stochastic. The solutions, or quantities of interests, are expressed as convergent series of orthogonal polynomial expansions in terms of the input random parameters. A high-order stochastic collocation method is employed to solve the solution statistics, and more importantly, to reconstruct the polynomial expansion. While retaining the high accuracy by polynomial expansion, the resulting "pseudo-spectral" type algorithm is straightforward to implement as it requires only repetitive deterministic simulations. An estimate on error bounded is presented, along with numerical examples for problems with relatively complicated forms of governing equations.

AMS subject classifications: 65C20, 65C30

Key words: Collocation methods, pseudo-spectral methods, stochastic inputs, random differential equations, uncertainty quantification.

1 Introduction

The focus of this paper is on efficient numerical methods for differential/algebraic equations with random/uncertain parameters. In the past years, this subject has received increasing amount of attention in a variety of engineering disciplines, especially those involving complex physics. In such complex fields, mathematical models can only serve as simplified and reduced representations of true physics, and there exists a significant amount of uncertainty associated with parameter values, boundary/initial conditions, constitutive laws, etc. For example, biochemical reactions are often modeled by (large) systems of ordinary differential equations (ODEs) or differential-algebraic equations (DAEs). Although these models have been successful in revealing quantitative connections between reaction details and observables, their usage is often constrained by the

*Corresponding author. *Email address:* dxiu@math.purdue.edu (D. Xiu)

difficulty of assigning numerical values to kinetic parameters (e.g., rate constants and binding constants) in the governing equations. Common approach is to conduct parameter estimation, in order to bring numerical solutions in reasonable agreement with a set of experimental observations. Because of the complexity of most biochemical processes and the diversity of the type of data to be fitted, the estimated model parameters usually contain significant uncertainties, rather than having precise numerical values. Traditional approach assigns "most likely" values to the parameters from their corresponding ranges, and such an approach could be inadequate as the complex biochemical processes may depend sensitively to some of the parameters. Also, very often observables from experiment measurements are not repeated enough times for reliable statistical estimates to be made on the "likelihood" of the parameter values. (General discussions on mathematical biology can be found in [6, 21], etc.) Therefore, mathematical and numerical techniques are needed to develop effective means of quantifying parameter uncertainty and its effect in complex systems.

In this paper we discuss an efficient method for parametric uncertainty analysis in (ordinary) differential-algebraic equations (DAEs). The uncertain parameters associated with the models are modeled as random variables. Subsequently, the resulting DAEs become stochastic equations. We remark that this type of stochastic systems are different from the classical "stochastic differential equations" (SDE) where the random inputs are some idealized processes such as Wiener processes, Poisson processes, etc., and tools such as stochastic calculus have been developed extensively and are still under active research. (See, for example, [9, 14, 15, 20].) In the problems considered in this paper, the random inputs are parameters modeled as random variables.

One of the most commonly used methods is Monte Carlo sampling (MCS), or one of its variants. Although MCS is straightforward to apply as it only requires repetitive executions of deterministic simulations, typically a large number of such executions are needed as the solution statistics converge relatively slowly, e.g., the mean value typically converges as $1/\sqrt{K}$ where K is the number of realizations [7]. The resulting statistical errors due to insufficient number of realizations can undermine the conclusions of uncertainty analysis such as the level of confidence in model selection and parameter estimates, etc. The need for large number of realizations for accurate results can incur excessive computational burden, especially for systems that are already computationally intensive in their deterministic settings.

A recently developed method, generalized polynomial chaos (gPC) [28, 30], belong to the class of non-sampling methods. With gPC, stochastic quantities are expressed as orthogonal polynomials of the input random parameters, and different types of orthogonal polynomials can be chosen to achieve better convergence. gPC expansion is essentially a spectral representation in random space, and exhibits fast convergence when the expanded function depends smoothly on the random parameters. Exponentially fast convergence can be achieved under certain circumstances. (See [2, 28] for detailed discussions.)

When applied to differential equations with random inputs, the quantities to be solved

are the expansion coefficients of the gPC expansion. A typical approach is to conduct a Galerkin projection to minimize the error of the finite-order gPC expansion, and the resulting set of equations for the expansion coefficients are deterministic and can be solved via conventional numerical techniques. This has been done in various applications and proved to be very effective [2, 8, 11, 16, 27–29]. However, stochastic Galerkin (SG) procedure can be challenging when the governing stochastic equations take complicated forms. In this case, the derivation of explicit equations for the gPC coefficients can be very difficult, if not impossible. To this end, high-order stochastic collocation (SC) approach is investigated in [26]. SC combines the advantages of both Monte Carlo sampling and gPC-Galerkin method. The implementation of a SC algorithm is similar to that of MCS, i.e., only repetitive realizations of a deterministic solver is required; and by choosing a set of nodes–“sampling points”–based on the theory of multivariate polynomial interpolations, it retains the high accuracy and fast convergence of gPC expansion, similar to SG.

It should be mentioned here that collocational approach to random equations is not a new idea. Also termed “deterministic sampling method”, it has been used in various engineering applications for a long time. (See, for example, [17, 24].) These earlier work typically use tensor products of one-dimensional quadrature points as “sampling points” and are not proper for problems with large number of random variables because of the exponential growth of the number of points. (Also see a discussion in Section 4.1.) While using tensor product construction, the recent work of [1] conducts the first rigorous error analysis for stochastic elliptic equations. On the other hand, the work of [26] is a first systematical attempt to avoid using tensor product constructions. Instead it employs the so-called “sparse grid” [23] to tackle problems with large number of random variables more efficiently.

This paper extends the work of [26]. Here we apply stochastic collocation method to DAEs with complicated forms of governing equations–problems that are difficult to solve via the gPC-SG approach. We will also address the issue of recovering the gPC polynomial expansions from SC solutions, which was not discussed in [26]. In this sense, the method resembles more to the “pseudo spectral” approach of classical deterministic spectral methods [4, 12]. An estimate of error bounded is also provided.

2 Problem setup

In this section, we present the mathematical framework of stochastic collocation methods.

2.1 Governing equations

Let us consider a system of (ordinary) differential algebraic equations (DAEs), for real numbers $T > t_0$,

$$\begin{cases} F(t, y, y', \dots, y^{(l)}, p) = 0, & t \in (t_0, T], \\ g(t_0, y(t_0), \dots, y^{(l)}(t_0), p) = 0, \end{cases} \quad (2.1)$$

where function g sets appropriate initial conditions at $t = t_0$. Here $y = (y_1, \dots, y_J) \in \mathbb{R}^J$, $J \geq 1$, are the *state variables*, and $p = (p_1, \dots, p_N) \in \mathbb{R}^N$, $N \geq 1$, are *parameters* of interests. We assume that these parameters (p_1, \dots, p_N) are mutually independent of each other. (In another word, there may exist additional parameters that either are functions of p , or are not of our interests in studying.) Let us also define a set of quantities

$$z = (z_1, \dots, z_K) \in \mathbb{R}^K = G(y) \quad (2.2)$$

as *observables*, or, quantities of interests. It is the dependency of these observables, z , upon the input parameters p that we are interested in. That is, we wish to establish (numerically) the functions $z = z(p)$, and quantify the effects of input uncertainty of p on output z .

2.2 Probabilistic framework

In what follows, we will adopt a probabilistic framework and model $p = (p_1, \dots, p_N)$ as a N -variate random vector with independent components in a properly defined probability space $(\Omega, \mathcal{A}, \mathcal{P})$, whose event space is Ω and is equipped with σ -algebra \mathcal{A} and probability measure \mathcal{P} .

Let $\rho_i : \Gamma_i \rightarrow \mathbb{R}^+$ be the probability density functions (PDF) of the random variable $p_i(\omega)$, $\omega \in \Omega$, and its image $\Gamma_i \equiv p_i(\Omega) \in \mathbb{R}$ be intervals in \mathbb{R} for $i = 1, \dots, N$. Then

$$\rho(p) = \prod_{i=1}^N \rho_i(p_i), \quad \forall p \in \Gamma \quad (2.3)$$

is the joint probability density of the random vector $p = (p_1, \dots, p_N)$ with the support

$$\Gamma \equiv \prod_{i=1}^N \Gamma_i \subset \mathbb{R}^N. \quad (2.4)$$

This allows us to conduct numerical formulations in the finite dimensional (N -dimensional) random space Γ , in replacement of the infinite dimensional space Ω . And the governing equation (2.1) should be valid for all $p \in \Gamma$. Naturally, the solution for (2.1) and the observables (2.2) are functions of the same set of random variables p , i.e.,

$$y = y(t; p), \quad z = G(y) = z(p). \quad (2.5)$$

Finally, we also assume that the random parameters have identical probability density functions $\rho_1 = \dots = \rho_N$.[†]

[†]This assumption is made for notational convenience and without loss of generality, because random variables with different PDFs can always be transformed, at least conceptually, to a same PDF via their cumulative density functions (CDF). In this case, one may consider the form of governing equation (2.1) already incorporates such a transformation.

3 Generalized polynomial chaos

For notational convenience, the presentation in this section is on scalar equation, i.e., $J=1$ in (2.1), and scalar observable, i.e. $K=1$ in (2.2). For system of equations ($J > 1$) and/or multiple observables ($K > 1$), the procedure is simply repeated for each component.

3.1 gPC expansion

In the finite dimensional random space Γ defined in (2.4), the gPC expansion seeks to approximate a random function via orthogonal polynomials of random variables. Let us define one-dimensional orthogonal polynomial spaces with respect to the measure $\rho_i(p_i)dy$ in Γ_i ,

$$W^{i,d_i} \equiv \left\{ v: \Gamma_i \rightarrow \mathbb{R}: v \in \text{span} \{ \phi_m(p_i) \}_{m=0}^{d_i} \right\}, \quad i=1, \dots, N, \quad (3.1)$$

where $\{ \phi_m(p_i) \}$ are a set of orthogonal polynomials satisfying the orthogonality conditions

$$\int_{\Gamma_i} \rho_i(p_i) \phi_m(p_i) \phi_n(p_i) dp_i = h_m^2 \delta_{mn}, \quad (3.2)$$

with normalization factors $h_m^2 = \int_{\Gamma_i} \rho_i \phi_m^2 dp_i$. With proper scaling, one can always normalize the bases such that $h_m^2 \equiv 1, \forall m$, and this shall be adopted throughout this paper. The type of the orthogonal polynomials $\{ \phi_m(p_i) \}$ in (3.4) is determined by $\rho_i(p_i)$, the probability density function, for $i=1, \dots, N$. For example, uniform distributions are associated with Legendre polynomials, and Gaussian distributions are associated with Hermite polynomials. (See [27,28] for a detailed list of correspondences.)

The corresponding N -variate orthogonal polynomial space in Γ is defined as

$$W_N^P \equiv \bigotimes_{|\mathbf{d}| \leq P} W^{i,d_i}, \quad (3.3)$$

where the tensor product is over all possible combinations of the multi-index $\mathbf{d} = (d_1, \dots, d_N) \in \mathbb{N}_0^N$ satisfying $|\mathbf{d}| = \sum_{i=1}^N d_i \leq P$. Thus, W_N^P is the space of N -variate orthonormal polynomials of total degree at most P , and its basis functions satisfy

$$\int_{\Gamma} \Phi_m(p) \Phi_n(p) \rho(p) dp \equiv \mathbb{E} [\Phi_m(p) \Phi_n(p)] = \delta_{mn}, \quad (3.4)$$

for all $1 \leq m, n \leq \dim(W_N^P) = \binom{N+P}{N}$, where δ_{mn} is the Kronecker delta function, and \mathbb{E} is the expectation operator. Such spaces are often employed in the (generalized) polynomial chaos expansions [11,27,29].

The finite order, P^{th} -order, gPC approximation of the observable z in (2.5) is

$$\mathbb{P}_N^P z \equiv z_N^P(p) = \sum_{m=1}^M \hat{z}_m \Phi_m(p), \quad M = \binom{N+P}{N}, \quad (3.5)$$

where \mathbb{P}_N^P is a projection operator of Γ onto W_N^P , and

$$\hat{z}_m = \mathbb{E}[z(p)\Phi_m(p)] = \int_{\Gamma} z(p)\Phi_m(p)\rho(p)dp, \quad m = 1, \dots, M. \quad (3.6)$$

Let

$$\epsilon_G \equiv \|z - \mathbb{P}_N^P z\|_{L^2_p(\Gamma)} = \left(\mathbb{E}[(z(p) - z_N^P(p))^2] \right)^{1/2} \quad (3.7)$$

be the mean square error of the finite-term gPC approximation, its convergence depends on the regularity of $z(p)$ and can be very fast when $z(p)$ is sufficiently smooth. Error analysis in tensor product polynomial space (not (3.3)) can be found in [1, 2].

3.2 Stochastic Galerkin

A typical approach to obtain numerical solution in the form of (3.5) is to employ a stochastic Galerkin approach. In this method, we seek an approximate solution

$$y_N^P(t; p) = \sum_{m=1}^M \hat{y}_m(t) \Phi_m(p) \quad (3.8)$$

satisfying (2.1) in the following weak form, for all $f(p) \in W_N^P$,

$$\begin{cases} \int_{\Gamma} \rho(p) F(t, y_N^P, (y_N^P)', \dots, (y_N^P)^{(l)}, p) f(p) dp = 0, & t \in (t_0, T], \\ \int_{\Gamma} \rho(p) g(t_0, y_N^P(t_0), \dots, (y_N^P)^{(l)}(t_0), p) f(p) dp = 0. \end{cases} \quad (3.9)$$

The resulting equations are a set of (coupled) *deterministic* DAEs for $\{\hat{y}\}$, and standard numerical techniques can be applied. Upon solving (3.9), the gPC approximation of the observable can be obtained as

$$u_N^P(p) = \sum_{m=1}^M \hat{u}_m \Phi_m(p), \quad \hat{u}_m = \int_{\Gamma} G(y_N^P) \Phi_m(p) \rho(p) dp. \quad (3.10)$$

Such a Galerkin procedure has been used extensively in the literature [2, 8, 11, 16, 27–29]. However, when (2.1) takes a complicated form, the derivation of Galerkin projection in (3.9), and subsequently the gPC approximation of the observable in (3.10), can become highly non-trivial, if not impossible. This is especially true when $z = G(y)$ does not have an explicit formulation, e.g., z is defined as the period of a limit cycle solution of y , etc. These are cases considered in this paper, and we employ the stochastic collocation method to circumvent the difficulty. Stochastic Galerkin methods will not be discussed.

4 Stochastic collocation algorithm

In stochastic collocational approach, we again seek an approximate solution to the observable z in the form of gPC expansion, similar to (3.5),

$$\mathbb{I}_N^P z \equiv v_N^P(t, p) = \sum_{m=1}^M \hat{v}_m(t) \Phi_m(p), \quad M = \binom{N+P}{N}, \tag{4.1}$$

where \mathbb{I} is another operator of Γ onto W_N^P , and

$$\hat{v}_m(t) = \sum_{j=1}^Q z(t, p^j) \Phi_m(p^j) \alpha_j, \quad m = 1, \dots, M. \tag{4.2}$$

Here $\{p^j, \alpha^j\}_{j=1}^Q$ are a set of nodes and weights, where $p^j = (p_1^j, \dots, p_N^j)$ and α^j denote the j -th node and its associated weights, respectively, in the N -variate space Γ such that

$$\mathcal{U}^Q[f] \equiv \sum_{j=1}^Q f(p^j) \alpha^j \tag{4.3}$$

is an approximation of integral

$$\mathcal{I}[f] \equiv \int_{\Gamma} f(p) \rho(p) dp = \mathbb{E}[f(p)] \tag{4.4}$$

for sufficiently smooth functions $f(p)$, i.e.,

$$\mathcal{U}^Q[f] \rightarrow \mathcal{I}[f], \quad Q \rightarrow \infty.$$

With such a choice of the nodal set, (4.2) approximates (3.6) such that

$$|\hat{v}_m - \hat{z}_m| = \left| (\mathcal{U}^Q - \mathcal{I})[z(p) \Phi_m(p)] \right|, \quad m = 1, \dots, M, \tag{4.5}$$

approaches zero as $Q \rightarrow \infty$. Subsequently, $\mathbb{I}_N^P u$ of (4.1) is an approximation of the true gPC expansion $\mathbb{P}_N^P u$ of (3.5), and its mean square error is defined as

$$\epsilon_Q \equiv \left\| \mathbb{I}_N^P z - \mathbb{P}_N^P z \right\|_{L^2_p(\Gamma)} = \left(\mathbb{E} \left[(\mathbb{I}_N^P - \mathbb{P}_N^P) z \right]^2 \right)^{1/2}. \tag{4.6}$$

This is what is commonly termed as ‘‘aliasing error’’ in classical deterministic spectral methods [4, 12].

4.1 Choices of nodal set

The key issue in SC method is the choice of the nodal set so that the integration rule (4.3) is accurate and efficient, especially in multivariate space Γ with $N > 1$. Many choices are available in one-dimensional space, i.e., $N = 1$. For every directions $i = 1, \dots, N$, we can construct a good one-dimensional integration rule

$$\mathcal{U}_i^{q_i}[f] = \sum_{j=1}^{q_i} f(p_i^j) \cdot \alpha_i^j, \quad (4.7)$$

based on nodal sets

$$\Theta_i^1 = (p_i^1, \dots, p_i^{q_i}) \subset \Gamma_i. \quad (4.8)$$

For sufficiently smooth integrand, one of the optimal choices is quadrature rules based on orthogonal polynomials $\{\phi_m(p_i)\}$ in (3.2).

4.1.1 Tensor products

In multivariate case $N > 1$, the tensor product formulas are

$$\mathcal{U}^Q[f] \equiv (\mathcal{U}_1^{q_1} \otimes \dots \otimes \mathcal{U}_N^{q_N})[f] = \sum_{j_1=1}^{q_1} \dots \sum_{j_N=1}^{q_N} f(p_1^{j_1}, \dots, p_N^{j_N}) \cdot (\alpha_1^{j_1} \otimes \dots \otimes \alpha_N^{j_N}). \quad (4.9)$$

Clearly, the above product formula needs $Q = \prod_{i=1}^N q_i$ nodal points. If we choose the same number of points in each dimension, i.e., $q_1 = \dots = q_N \equiv q$, the total number of points is $Q = q^N$. This number grows quickly in high dimensions $N \gg 1$ – for a modest approximation with three points ($q=3$) in each dimension, $Q=3^N \gg 1$ for $N \gg 1$ (e.g., for $N=10$, $3^{10} \sim 6 \times 10^4$). Because of the rapidly growing number of nodes in high dimensions, it is proper to consider tensor product approach only for lower dimensions, e.g., $N \leq 5$.

4.1.2 Sparse grids

Sparse grids were first proposed in [23], and it was found to be particularly useful in solving random differential equations by stochastic collocation approach in high dimensional random spaces [26]. The Smolyak algorithm is a linear combination of product formulas, and the linear combination is chosen in such a way that an integration property for $N=1$ is preserved for $N > 1$ as much as possible. Only products with a relatively small number of points are used and the resulting nodal set has significantly less number of nodes compared to the tensor product rule (4.9). Much research has been devoted to the Smolyak algorithm since its introduction, see, e.g., [3, 18, 19], etc.

Starting with the one-dimensional integration formula (4.7), the Smolyak algorithm is given by (see [25])

$$\mathcal{U}^Q(f) \equiv A(J, N) = \sum_{J-N+1 \leq |\mathbf{i}| \leq J} (-1)^{J-|\mathbf{i}|} \binom{N-1}{J-|\mathbf{i}|} \cdot (\mathcal{U}_{i_1} \otimes \dots \otimes \mathcal{U}_{i_N}), \quad (4.10)$$

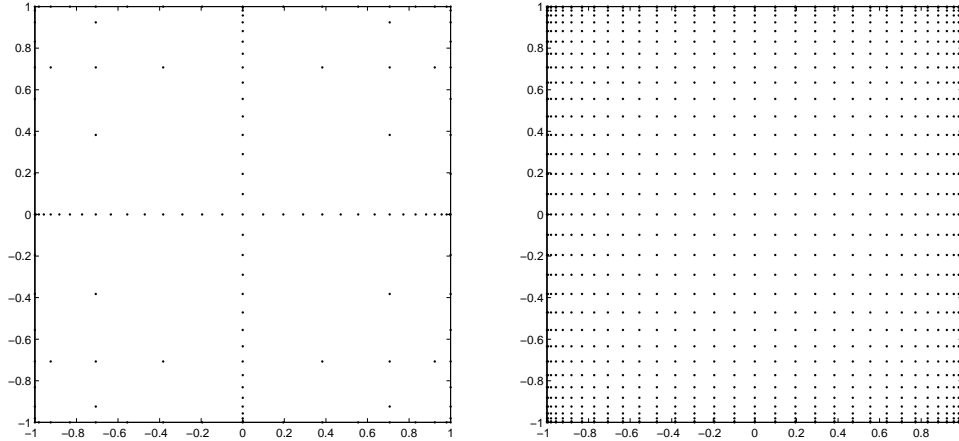


Figure 1: Two-dimensional ($N=2$) nodes based on the extrema of Chebyshev polynomials (4.12). Left: Sparse grid $\mathcal{H}(N+k, N)$ from Smolyak algorithm, $k=5$. Total number of points is 145. Right: Tensor product algorithm (4.9) from the same one-dimensional nodes. Total number of nodes is 1,089.

where $\mathbf{i} = (i_1, \dots, i_N) \in \mathbb{N}^N$. To compute $A(J, N)$, we only need to evaluate function on the “sparse grid”

$$\Theta_N \equiv \mathcal{H}(J, N) = \bigcup_{J-N+1 \leq |\mathbf{i}| \leq J} (\Theta_{i_1}^1 \times \dots \times \Theta_{i_N}^1). \quad (4.11)$$

In this paper, we use extensively the Smolyak formulas based on one-dimensional polynomial integration at the extrema of the Chebyshev polynomials. (Other Gauss quadrature points, can be considered as well.) For any choice of $q_i > 1$, these nodes are given by

$$p_i^j = -\cos \frac{\pi(j-1)}{q_i-1}, \quad j=1 \dots, q_i. \quad (4.12)$$

In addition, we define $p_i^1 = 0$ if $q_i = 1$ and choose $q_1 = 1$ and $q_i = 2^{i-1} + 1$ for $i > 1$. By doing so, the one-dimensional nodal sets Θ_i^1 are nested, and subsequently $\mathcal{H}(J, N) \subset \mathcal{H}(J+1, N)$. It can be shown that, if we set $J = N + P$, then $A(N + P, N)$ is exact for integration of polynomials in a space larger than W_N^P ([18]), and the total number of nodes for $N \gg 1$ satisfies

$$Q \equiv \dim(A(N + P, N)) \sim \frac{2^P}{P!} N^P, \quad P \text{ fixed}, N \gg 1. \quad (4.13)$$

The dependence on dimension N is much weaker than tensor product rule. Since $\dim(W_N^P) = \binom{N+P}{N} \sim N^P / P!$ for $N \gg 1$, $Q \sim 2^P \dim(W_N^P)$ for $N \gg 1$ and the factor is independent of dimension N . Hereafter, we will refer k in $A(N+k, N)$ as the “level” of the sparse grid integration. An example of two-dimensional ($N=2$) nodes by the sparse grid $\mathcal{H}(N+k, N)$ with $k=5$ is shown in Fig. 1, along with the tensor product grid based on the same one-dimensional nodes. We observe that the sparse grid has significantly less number of nodes.

For details on construction and properties of sparse grid, see [3, 18, 19] and the reference therein.

4.1.3 Other choices

Other choices of nodal set can be sought for (4.3). For example, one can employ Monte Carlo method, where the nodes are randomly generated and $\omega^j \equiv 1/Q$, $j = 1, \dots, Q$. However, the (relatively) larger statistical errors due to the (relatively) slower convergence of Monte Carlo method may incur large aliasing errors (4.6) which can negate the fast convergence property offered by gPC expansion. Therefore, we will not consider Monte Carlo integration in this paper. We remark that multivariate integration remains an active research field and there are many other choices of nodal sets. (See [5, 13] for an review.) Here we only focus on the sparse grid construction because, by using an accurate one-dimensional quadrature rule, it offers systematical accuracy refinement to arbitrary polynomial orders in multivariate spaces.

4.2 Algorithm summary

The stochastic collocation algorithm for the DAE system (2.1) and (2.2) consists of the following steps:

1. Choose a collocation nodal set $\{p^j, \omega^j\}_{j=1}^Q$ in space Γ ;
2. for each $j = 1, \dots, Q$, solve problem (2.1) with a fixed parameter set $p^j = (p_1^j, \dots, p_N^j)$, via an accurate numerical scheme, to obtain its solution $\tilde{y}(p^j)$, and evaluate the observables $\tilde{z}(p^j) = G(\tilde{y}(p^j))$; (Note this is a deterministic problem.)
3. evaluate the approximate gPC expansion coefficients

$$\hat{w}_m = \mathcal{U}^Q[\tilde{z}(p)\Phi_m(p)] = \sum_{j=1}^Q \tilde{z}(p^j)\phi_m(p^j)\omega^j, \quad m = 1, \dots, M; \quad (4.14)$$

4. and finally, construct the N -variate, P -th order gPC approximation

$$w_N^P = \sum_{m=1}^M \hat{w}_m \Phi_m(p), \quad M = \binom{N+P}{N}. \quad (4.15)$$

We remark that the major computational efforts will likely be on the repetitive and *deterministic* solutions of (2.1)–(2.2) for each fixed parameters p^j , $j = 1, \dots, Q$. The choice of nodal set is a pre-processing step, and the evaluation of gPC coefficients (4.14) and reconstruction of the approximate gPC expression (4.15) are post-processing steps. It also should be noted that an accurate estimation of the gPC coefficients via an integration rule (4.14) is critical in obtained an accurate gPC representation. Therefore, sufficiently large number of points (Q) should be used for a given integration rule to ensure the accuracy of (4.14).

4.3 Error separation

Let us assume that an accurate and stable numerical scheme is employed for the deterministic problem (2.1)–(2.2) with fixed parameter p^j and the error of its numerical solution $\tilde{z}(p^j)$ is

$$\epsilon_\Delta \equiv \max_j \epsilon_\Delta^j = \max_j |z(p^j) - \tilde{z}(p^j)|, \quad j=1, \dots, Q, \tag{4.16}$$

where Δ denotes the set of discretizational parameters, e.g., time steps, etc.

Let us also define

$$\gamma_m^Q = \mathcal{U}^Q[\Phi_m(p)] = \begin{cases} 1 & m=1, \\ \mathcal{U}^Q[\Phi_m(p)] & m \neq 1. \end{cases} \tag{4.17}$$

The last term follows the fact that $\Phi_1(p) \equiv 1$ and all integration rule should satisfy $\mathcal{U}[1] = \mathcal{I}[1] = 1$. Also, $\gamma_m^Q \approx \mathcal{I}[\Phi_m(p)] = 0$ for all $m \neq 1$. And if an integration rule is chosen to be exact for all polynomials in W_N^P , $\gamma_m^Q = 0$ for all $m \neq 1$.

Proposition 4.1 (Error superposition). Let ϵ_Δ , defined in (4.16), be the error induced by solving the deterministic problem (2.1)–(2.2); ϵ_Q be the aliasing error of approximating the gPC expansions via a given integration rule, as defined in (4.6); and γ_m^Q be defined in (4.17), then the mean-square error of N -variate, P -th order gPC stochastic collocation solution w_N^P , defined in (4.15), satisfies

$$\epsilon = \left(\int_\Gamma [z(p) - w_N^P(p)]^2 \rho(p) dp \right)^{1/2} \leq [\epsilon_G^2 + \epsilon_Q^2 + M\epsilon_\Delta^2 C_Q^2]^{1/2}, \tag{4.18}$$

where $C_Q = \max_m |\gamma_m^Q|$, and ϵ_G is the mean square error of finite-term gPC projection (3.7).

Proof. Observe that

$$\begin{aligned} \epsilon^2 &\equiv \int_\Gamma [z(p) - w_N^P(p)]^2 \rho(p) dp \\ &\leq \int_\Gamma [z - \mathbb{P}_N^P z]^2 \rho(p) dp + \int_\Gamma [\mathbb{P}_N^P z - \mathbb{I}_N^P z]^2 \rho(p) dp + \int_\Gamma [\mathbb{I}_N^P z - w_N^P]^2 \rho(p) dp \\ &= \epsilon_G^2 + \epsilon_Q^2 + \int_\Gamma [v_N^P(p) - w_N^P(p)]^2 \rho(p) dp. \end{aligned}$$

The last term is

$$\begin{aligned} \int_\Gamma [v_N^P(p) - w_N^P(p)]^2 \rho(p) dp &= \int_\Gamma \left[\sum_{m=1}^M (\hat{v}_m - \hat{w}_m) \Phi_m(p) \right]^2 \rho(p) dp \\ &= \sum_{m=1}^M (\hat{v}_m - \hat{w}_m)^2 = \sum_{m=1}^M \left[\sum_{j=1}^Q (z(p^j) - \tilde{z}(p^j)) \Phi_m(p^j) \alpha^j \right]^2 \\ &\leq \epsilon_\Delta^2 M \cdot \max_m \left[\sum_{j=1}^Q \Phi_m(p^j) \alpha^j \right]^2 = \epsilon_\Delta^2 M C_Q^2, \end{aligned}$$

where the orthogonality of the basis functions (3.4) have been used. This completes the proof. \square

We remark that with a proper integration rule $\gamma_m^Q \approx \mathcal{I}[\Phi_m(p)] = \delta_{m1}, \forall m$, if not exactly, and $C_Q = 1$. The result demonstrates that the overall error of the SC algorithm can be roughly characterized into three contributions: ϵ_G , the projection error due to the finite-term gPC expansion (3.7); ϵ_Q , the aliasing error (4.6) by the Q -point integration rule (4.3); and ϵ_Δ , the error introduced by solving (2.1)–(2.2) with fixed parameters by a numerical scheme with discretizational parameters Δ . All of these errors can be controlled in practice, and can be refined by increasing the order of gPC expansion, integration rule, and numerical scheme, respectively, provided that the observable $z(p)$ is sufficiently smooth.

5 Numerical examples

In this section we present several numerical examples to demonstrate the efficiency and accuracy of the SC algorithm. In all results, numerical errors of the deterministic solvers for (2.1)–(2.2) are negligible. The focus is on the flexibility of the algorithm to problems with complex form.

5.1 A model problem

Here we set the observables with the following explicit definition

$$\begin{aligned} z_1 &= p_1 \cdot e^{p_2} / (1 + p_3^2), \\ z_2 &= \cos(p_1) \ln \left(\frac{1}{2} + p_2^2 + p_3^2 \right), \end{aligned} \quad (5.1)$$

where $p = (p_1, p_2, p_3)$ are three independent Gaussian random variables with zero mean and standard deviation $\sigma = 0.1$. This can be considered as an exact solution to certain differential equations whose dependence in physical space/time has been suppressed. Therefore, the deterministic numerical error ϵ_Δ (4.16) is eliminated. Corresponding the Gaussian distribution, the gPC basis functions are Hermite polynomials. The random space is three-dimensional ($N = 3$), and we adopt tensor product of one-dimensional Hermite quadrature as integration rule. Each dimension has the same number of node, $q = q_1 = q_2 = q_3$, and the total number of nodes is $Q = q^3$.

The mean square errors of z_1 and z_2 are shown in Fig. 2. The numbers of integration node are $q = 2$, $q = 4$, and $q = 6$. It can be seen that as the order of gPC expansion (P) is increased, the errors converge only when sufficient number integration nodes are employed—near exponential convergence offered by gPC is achieved only when aliasing error is sufficiently small (with $q = 6$). Larger aliasing error cause the error to saturate ($q = 4$), and it is particularly significant at higher gPC orders when a poor integration resolution ($q = 2$) is used.

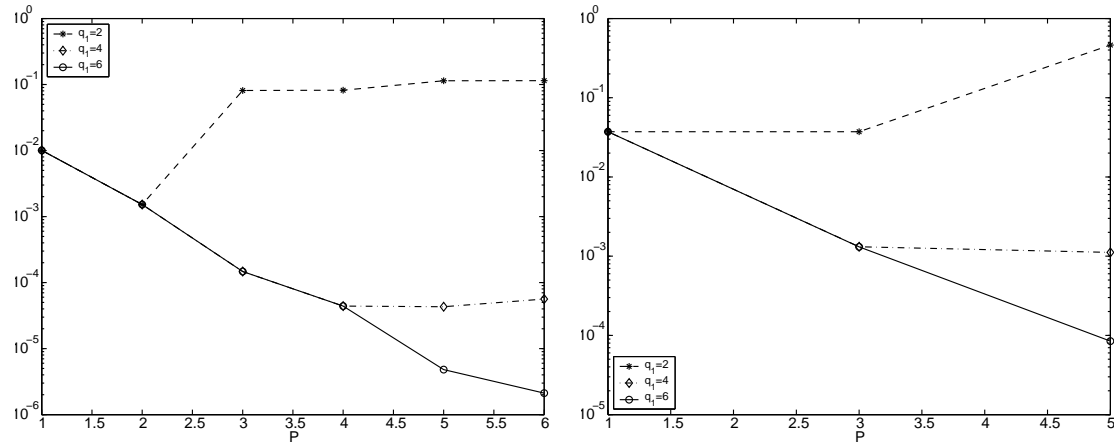


Figure 2: Mean-square error of model problem (5.1), with increasing order of gPC expansion and different number of integration nodes in each dimension. Left: errors in z_1 ; Right: errors in z_2 .

More numerical demonstration of the gPC convergence can be found in the gPC-Galerkin literature [27–29].

5.2 Genetic toggle switch

Here we consider a model for a genetic toggle switch in *Escherichia coli*, which was constructed in [10]. It is composed of two repressors and two constitutive promoters, where each promoter is inhibited by the repressor that is transcribed by the opposing promoter. Details of experimental measurement can be found in [10], where the following dimensionless model, derived from a biochemical rate equation formulation of gene expression [6,21], was also proposed,

$$\frac{du}{dt} = \frac{\alpha_1}{1+v^\beta} - u, \quad (5.2)$$

$$\frac{dv}{dt} = \frac{\alpha_2}{1+w^\gamma} - v, \quad (5.3)$$

$$w = \frac{u}{(1+[\text{IPTG}]/K)^\eta}. \quad (5.4)$$

This is an ordinary differential-algebraic (DAE) system, with six parameters $p = (\alpha_1, \alpha_2, \beta, \gamma, \eta, K)$ and input function [IPTG]. The values of these parameters are highly uncertain, and they are estimated as deterministic in [10]. Here we set the parameters as $p = \langle p \rangle (1 + \sigma y)$ where the mean $\langle p \rangle = (156.25, 15.6, 2.5, 1, 2.0015, 2.9618 \times 10^{-5})$, $\sigma = 0.1$, and y is random vector uniformly distributed in $(-1, 1)^6$ with independent components. Corresponding the uniform distribution, the gPC basis are Legendre polynomials. The random space is six-dimensional ($N=6$), and the sparse grids are employed as integration rule. Resolution check is conducted, and it is found that second-order gPC ($P=2$) expansion with third-level sparse grids are sufficient. The solution curve of normalized v is shown in error

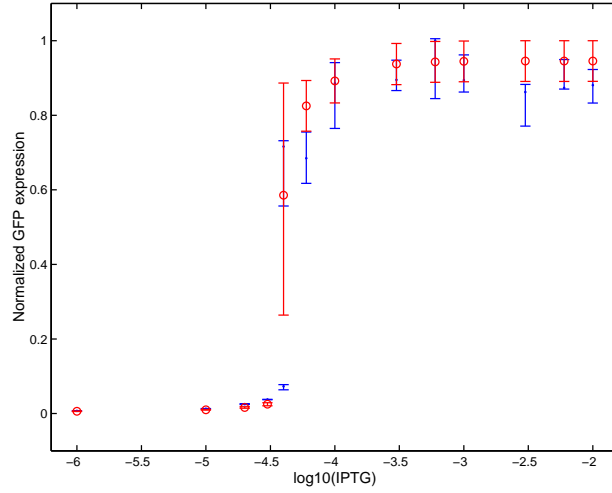


Figure 3: Steady-state gene expression of toggle swith. Light (and red) error bars centered around circles are numerical results; Dark (and blue) error bars around dots are experimental measurements. The re-production of the experimental results from [10] is courtesy of Dr.Gardner.

bars with respect to varying IPTG input. We observe good agreement between numerical error bars (light-colored bars around circles) and experimental error bars (dark-colored bars around dots). The switch property is indicated by the sudden jump in the response curve. At this location, the solution has a bi-modal distribution, indicated by the larger numerical error bar. (The experimental result at this location is plotted as two smaller bars corresponding to each modal.) We remark that the form of the governing equations prevents direct application of gPC-Galerkin approach.

5.3 Cell signaling cascade

Here we consider a mathematical model for autocrine cell-signaling loop developed in [22]. Let e_{1p} , e_{2p} , and e_{3p} denote the dimensionless concentrations of the active form of the enzymes. The model for dynamics of e_{1p} , e_{2p} , and e_{3p} has the following form

$$\frac{de_{1p}}{dt} = \frac{I(t)}{1 + G_4 e_{3p}} \frac{V_{\max,1}(1 - e_{1p})}{K_{m,1} + (1 - e_{1p})} - \frac{V_{\max,2} e_{1p}}{K_{m,2} + e_{1p}}, \quad (5.5)$$

$$\frac{de_{2p}}{dt} = \frac{V_{\max,3} e_{1p}(1 - e_{2p})}{K_{m,3} + (1 - e_{2p})} - \frac{V_{\max,4} e_{2p}}{K_{m,4} + e_{2p}}, \quad (5.6)$$

$$\frac{de_{3p}}{dt} = \frac{V_{\max,5} e_{2p}(1 - e_{3p})}{K_{m,5} + (1 - e_{3p})} - \frac{V_{\max,6} e_{3p}}{K_{m,6} + e_{3p}}. \quad (5.7)$$

For detailed biological background of the model, see [22]. In [22], the parameters are chosen as $K_{m,1-6} = 0.2$, $V_{\max,1} = 0.5$, $V_{\max,2} = 0.15$, $V_{\max,3} = 0.15$, $V_{\max,4} = 0.15$, $V_{\max,5} = 0.25$, and $V_{\max,6} = 0.05$, and the response curve of e_{3p} with respect to the input signal $I(t)$ is examined at steady state.

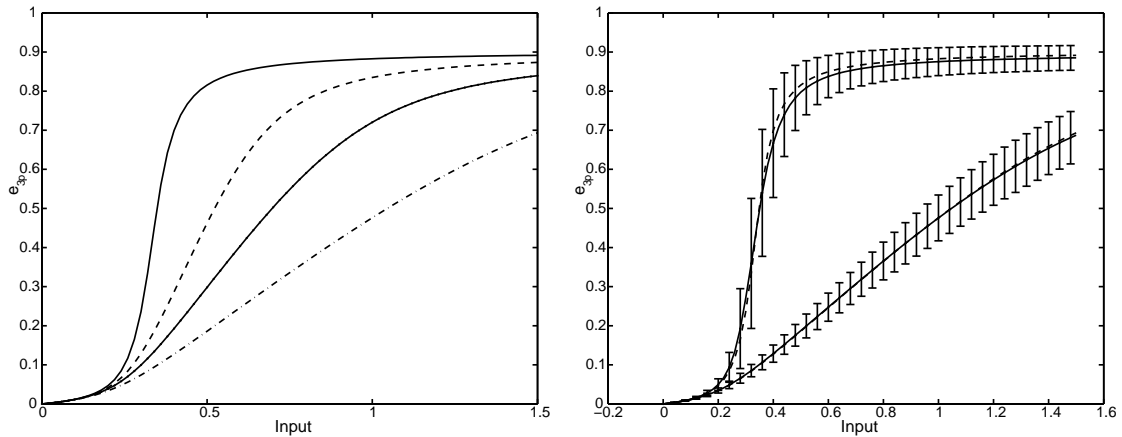


Figure 4: Steady input-out behavior computed for several values for gain of the negative feedback Left: deterministic simulation. The four curves from top to bottom correspond to $G_4=0,1,2$, and 4 , respectively. Right: stochastic computation with 10% uncertainty in parameters $V_{\max,1-6}$. Results of $G_4=0$ and $G_4=4$ are shown in error bars, with the corresponding deterministic results in dotted lines.

Here we introduce 10% uncertainty in the parameters $V_{\max,1-6}$ to account for the data variability, and model these parameter as, for $i=1, \dots, 6$, $V_{\max,i} = \langle V_{\max,i} \rangle (1 + \sigma p_i)$, where $\sigma = 0.1$, p_i is a uniformly distributed random variable in $(-1,1)$, and the mean values $\langle V_{\max,i} \rangle$ are specified as the same values above. Again, the gPC basis functions are Legendre polynomials for uniform random variables. The random space is six-dimensional ($N=6$), and the sparse grids are used.

The left of Fig. 4 is the result of deterministic simulations, with the four curves corresponds to $G_4=0,1,2$, and 4 , from top to bottom, respectively. This is a reproduction of Figure 4 in [22]. The steady input-output behavior with random parameters for $G_4=0$ and $G_4=4$ is plotted on the right of Fig. 4, in error bars to illustrate the uncertainty in output induced by the uncertainty in parameters. (The corresponding base case deterministic results are plotted in dashed lines.) It can be seen that although the difference between the mean of the random output and the deterministic output is quite small, relatively large output uncertainty (indicated by error bars) is obtained when the response curve has larger slope.

For smaller values of G_4 , the stimulus-response curve takes the form of the Hill equation $y = x^{n_h} / (\bar{x}^{n_h} + x^{n_h})$, where n_h is the Hill coefficient and \bar{x} represent the value of x where $y = 1/2$. The Hill coefficient is often approximated by

$$n_h = \frac{\log(81)}{\log(I_{90}/I_{10})}, \tag{5.8}$$

where I_{90} and I_{10} represent the input value that result in 90% and 10% of output activity, respectively. Here we take n_h as another observable and examine it for the response curve of $G_4=0$. It is shown that the mean of n_h is 6.4682 and its standard deviation is 0.775.

Furthermore, the approximate gPC expansion (4.15) of n_h is constructed

$$n_h = \langle n_h \rangle + \sum_{k=1}^6 \hat{w}_k p_k + \text{high order terms}, \quad (5.9)$$

with

$$\begin{aligned} \hat{w}_1 &= -0.0352, & \hat{w}_2 &= 0.0362, & \hat{w}_3 &= 0.8976, \\ \hat{w}_4 &= -0.8981, & \hat{w}_5 &= 0.2918, & \hat{w}_6 &= -0.2901. \end{aligned}$$

Note that \hat{w}_k is the leading term in $\partial n_h / \partial p_k$, for $k = 1, \dots, 6$. Therefore, it is a measure of *output sensitivity* with respect to the input parameters p_k . The above result indicates that the Hill coefficient is not sensitive to data uncertainty in parameters $V_{\max,1}$ and $V_{\max,2}$, and is highly sensitive to $V_{\max,3}$ and $V_{\max,4}$. Note that the Hill coefficient (5.8) does not have an explicit definition with respect to input parameters and it is difficult to obtain an approximate gPC expansion of (5.9) via a Galerkin approach.

6 Summary

In this paper the high-order stochastic collocation (SC) method, first examined systematically in [1,26], is combined with the generalized polynomial chaos (gPC) expansion [28]. The resulting algorithm is a pseudo-spectral type approach, where the issue of reconstructing the gPC expansion is addressed. The overall algorithm is straightforward to implement, as it requires only repetitive deterministic solvers like Monte Carlo approach, and with proper integration rule for polynomial reconstruction, it retains fast convergence of gPC expansion. Several numerical examples are presented for differential-algebraic equations with complex form, where a gPC-Galerkin approach is difficult to apply.

It is shown that the error of SC-gPC approach can be decomposed into three parts: the projection error of gPC expansion, the aliasing error of integration rule, and the numerical error of deterministic solver. Several choices of integration points are discussed, and the sparse grid construction appears to be a reasonable choice for problems with moderately large number of random variables.

References

- [1] I. Babuška, F. Nobile and R. Tempone, A stochastic collocation method for elliptic partial differential equations with random input data, *SIAM J. Numer. Anal.*, to appear.
- [2] I. Babuška, R. Tempone and G. Zouraris, Galerkin finite element approximations of stochastic elliptic differential equations, *SIAM J. Numer. Anal.*, 42 (2004), 800-825.
- [3] V. Barthelmann, E. Novak and K. Ritter, High dimensional polynomial interpolation on sparse grid, *Adv. Comput. Math.*, 12 (1999), 273-288.
- [4] C. Canuto, M. Hussaini, A. Quarteroni and T. Zang, *Spectral Method in Fluid Dynamics*, Springer-Verlag, New York, 1988.
- [5] R. Cools, An encyclopaedia of cubature formulas, *J. Complexity*, 19 (2003), 445-453.
- [6] L. Edelstein-Keshet, *Mathematical Models in Biology*, McGraw-Hill, New York, 1988.

- [7] G. Fishman, Monte Carlo: Concepts, Algorithms, and Applications, Springer-Verlag, New York, 1996.
- [8] P. Frauenfelder, C. Schwab and R. Todor, Finite elements for elliptic problems with stochastic coefficients, *Comput. Meth. Appl. Mech. Eng.*, 194 (2005), 205-228.
- [9] C. Gardiner, Handbook of Stochastic Methods: for Physics, Chemistry and the Natural Sciences, 2nd ed., Springer-Verlag, 1985.
- [10] T. Gardner, C. Cantor and J. Collins, Construction of a genetic toggle switch in *Escherichia coli*, *Nature*, 403 (2000), 339-342.
- [11] R. Ghanem and P. Spanos, Stochastic Finite Elements: A Spectral Approach, Springer-Verlag, 1991.
- [12] D. Gottlieb and S. Orszag, Numerical Analysis of Spectral Methods: Theory and Applications, SIAM-CMBS, Philadelphia, 1997.
- [13] S. Haber, Numerical evaluation of multiple integrals, *SIAM Rev.*, 12 (1970), 481-526.
- [14] I. Karatzas and S. Shreve, Brownian Motion and Stochastic Calculus, Springer-Verlag, New York, 1988.
- [15] P. Kloeden and E. Platen, Numerical Solution of Stochastic Differential Equations, Springer-Verlag, New York, 1999.
- [16] O. Le Maitre, O. Knio, H. Najm and R. Ghanem, Uncertainty propagation using Wiener-Haar expansions, *J. Comput. Phys.*, 197 (2004), 28-57.
- [17] L. Mathelin and M. Hussaini, A stochastic collocation algorithm for uncertainty analysis, Tech. Report NASA/CR-2003-212153, NASA Langley Research Center, 2003.
- [18] E. Novak and K. Ritter, High dimensional integration of smooth functions over cubes, *Numer. Math.*, 75 (1996), 79-97.
- [19] E. Novak and K. Ritter, Simple cubature formulas with high polynomial exactness, *Constr. Approx.*, 15 (1999), 499-522.
- [20] B. Oksendal, Stochastic Differential Equations: An Introduction with Applications, 5th ed., Springer-Verlag, New York, 1998.
- [21] S. Rubinow, Introduction to Mathematical Biology, Wiley, New York, 1975.
- [22] S. Shvartsman, M. Hagan, A. Yacoub, P. Dent, H. Wiley and D. Lauffenburger, Autocrine loops with positive feedback enable context-dependent cell signaling, *Am. J. Physiol.-Cell Physiol.*, 282 (2002), C545-C559.
- [23] S. Smolyak, Quadrature and interpolation formulas for tensor products of certain classes of functions, *Soviet Math. Dokl.*, 4 (1963), 240-243.
- [24] M. Tatang, W. Pan, R. Prinn and G. McRae, An efficient method for parametric uncertainty analysis of numerical geophysical model, *J. Geophys. Res.*, 102 (1997), 21925-21932.
- [25] G. Wasilkowski and H. Wozniakowski, Explicit cost bounds of algorithms for multivariate tensor product problems, *J. Complexity*, 11 (1995), 1-56.
- [26] D. Xiu and J. Hesthaven, High-order collocation methods for differential equations with random inputs, *SIAM J. Sci. Comput.*, 27 (2005), 1118-1139.
- [27] D. Xiu and G. Karniadakis, Modeling uncertainty in steady state diffusion problems via generalized polynomial chaos, *Comput. Methods Appl. Mech. Engrg.*, 191 (2002), 4927-4948.
- [28] D. Xiu and G. Karniadakis, The Wiener-Askey polynomial chaos for stochastic differential equations, *SIAM J. Sci. Comput.*, 24 (2002), 619-644.
- [29] D. Xiu and G. Karniadakis, Modeling uncertainty in flow simulations via generalized polynomial chaos, *J. Comput. Phys.*, 187 (2003), 137-167.
- [30] D. Xiu and J. Shen, An efficient spectral method for acoustic scattering from rough surfaces, *Commun. Comput. Phys.*, 2 (2007), 54-72.